Plant, Cell & Environment

Plant, Cell and Environment (2015) **38**, 2048–2060 doi: 10.1111/pce.12530

Original Article

Climate change alters leaf anatomy, but has no effects on volatile emissions from arctic plants

Michelle Schollert[1,2], Minna Kivimäenpää[3], Hanna M. Valolahti[1,2] & Riikka Rinnan[1,2]

[1]Terrestrial Ecology Section, Department of Biology, University of Copenhagen, Copenhagen Ø 2100, Denmark, [2]Center for Permafrost (CENPERM), Department of Geosciences and Natural Resource Management, University of Copenhagen, Copenhagen K 1350, Denmark and [3]Department of Environmental Science, University of Eastern Finland, Kuopio 70211, Finland

ABSTRACT

Biogenic volatile organic compound (BVOC) emissions are expected to change substantially because of the rapid advancement of climate change in the Arctic. BVOC emission changes can feed back both positively and negatively on climate warming. We investigated the effects of elevated temperature and shading on BVOC emissions from arctic plant species *Empetrum hermaphroditum*, *Cassiope tetragona*, *Betula nana* and *Salix arctica*. Measurements were performed *in situ* in long-term field experiments in subarctic and high Arctic using a dynamic enclosure system and collection of BVOCs into adsorbent cartridges analysed by gas chromatography-mass spectrometry. In order to assess whether the treatments had resulted in anatomical adaptations, we additionally examined leaf anatomy using light microscopy and scanning electron microscopy. Against expectations based on the known temperature and light-dependency of BVOC emissions, the emissions were barely affected by the treatments. In contrast, leaf anatomy of the studied plants was significantly altered in response to the treatments, and these responses appear to differ from species found at lower latitudes. We suggest that leaf anatomical acclimation may partially explain the lacking treatment effects on BVOC emissions at plant shoot-level. However, more studies are needed to unravel why BVOC emission responses in arctic plants differ from temperate species.

Key-words: *Betula nana*; *Cassiope tetragona*; *Empetrum hermaphroditum*; *Salix arctica*; BVOC; isoprenoid; microscopy; shading; temperature; warming.

INTRODUCTION

Over the last three decades, the Arctic has had a warming trend of about 1 °C per decade, which is significantly greater than the global mean (IPCC 2013). Also in the future, the Arctic region is projected to experience pronounced effects of the rapidly advancing climate warming (IPCC 2013), which impose substantial changes in the environment. As emissions of biogenic volatile organic compounds (BVOCs) from plants are highly temperature sensitive (Laothawornkitkul *et al*. 2009; Grote *et al*. 2013), drastically increased emissions from arctic plants are expected under the projected arctic warming of 3–11 °C by 2100 (IPCC 2013).

Alterations in BVOC emissions are of great interest as they contribute to complex climate feedback mechanisms via both positive and negative indirect effects on climate warming (Arneth *et al*. 2010; Kulmala *et al*. 2013). They prolong the atmospheric lifetime of methane (CH_4) and function as precursors of secondary organic aerosols (SOAs) possibly affecting cloud cover (Laothawornkitkul *et al*. 2009; Kulmala *et al*. 2013). Locally, BVOCs released by vegetation are involved in plant defence, growth, development and communication (Laothawornkitkul *et al*. 2009). Furthermore, BVOCs, in particular isoprene, are known for their protection against abiotic stresses (Vickers *et al*. 2009; Loreto & Schnitzler 2010; Possell & Loreto 2013). It is urgent to investigate how BVOC emissions from arctic plants respond to the predicted changes in climate.

Even high arctic heaths, dominated by dwarf shrubs or graminoids, have shown to be a source of various BVOCs and to have emissions that cannot be ignored (Schollert *et al*. 2014). However, relative to the global BVOC emissions, the emissions are likely to be low due to the scarce emitting plant biomass and short growing seasons (Rinnan *et al*. 2014). Besides being subjected to warming, which is likely to considerably increase the emissions (Tiiva *et al*. 2008; Faubert *et al*. 2010), the Arctic will also experience changes in precipitation, evaporation patterns and cloud cover (IPCC 2013). Increased cloudiness at high latitudes would potentially reduce the solar radiation reaching the Earth's surface (Stanhill & Cohen 2001; IPCC 2013). As emissions of many BVOCs are light-dependent (Laothawornkitkul *et al*. 2009; Monson & Baldocchi 2014a), reduced incoming radiation has the potential to decrease the emissions. Here, we examine how experimental warming and shading affect BVOC emissions from common arctic plant species.

Studies from the subarctic have shown experimental warming by 2–3 °C to increase the BVOC emissions at ecosystem level by as much as 50–250% depending on the compound and the year (Tiiva *et al*. 2008; Faubert *et al*. 2010). However, the mechanisms for these drastic increases, especially at the level of individual plants, are not understood. The

Correspondence: M. Schollert. e-mail: mschollert@bio.ku.dk

© 2015 The Authors. *Plant, Cell & Environment* published by John Wiley & Sons Ltd.
This is an open access article under the terms of the Creative Commons Attribution License, which permits use, distribution and reproduction in any medium, provided the original work is properly cited.

general positive short-term temperature response is due to the accelerated chemical reaction rates, higher volatility of stored compounds and increased cellular diffusion rates (Laothawornkitkul *et al*. 2009).

BVOC emission rates are largely driven by the temperature and light levels prevailing during the measurements, although the temperature of a preceding time period might also influence the emission rates as observed for isoprene (Potosnak *et al*. 2013). Methods indicative of BVOC synthesis rates, for example enzyme availability, gene expression or substrate availability could not be used in the remote locations because of logistical constraints. Instead, we assessed long-term acclimation to elevated temperature and shading by analysis of leaf anatomy by light and scanning electron microscopy, because leaf function and structure are interconnected.

Warming has been shown to induce anatomical changes in both deciduous and conifer trees, such as thinning of leaves/needles and leaf tissues, and larger leaf size (Higuchi *et al*. 1999; Luomala *et al*. 2005; Hartikainen *et al*. 2009, 2014). Hartikainen *et al*. (2009) suggested that warming-induced thinner leaves, with shorter diffusion pathways for BVOCs, could be linked to increased BVOC emissions from *Populus tremula* under warming. Recently, Rasulov *et al*. (2014) showed that leaf structural modifications were the primary reasons for temperature acclimation of photosynthesis and isoprene emission of hybrid aspen (*P. tremula* × *Populus tremuloides*). Shade-adapted leaves are also usually thinner than sun-adapted leaves (Larcher 2003) and have a lower net photosynthesis and thus a potentially reduced synthesis of BVOCs (Loreto & Schnitzler 2010; Li & Sharkey 2013). Both warming (Hartikainen *et al*. 2014) and shading (Marques *et al*. 1999) have been shown to reduce the density of trichomes, which are specialized storage structures for BVOCs (Loreto & Schnitzler 2010; Fineschi *et al*. 2013). Climate change factors can also alter stomatal density (Beerling & Chaloner 1993; Luomala *et al*. 2005), which can exert at least short-term control over BVOC emissions (see Niinemets & Reichstein 2003). It is largely unknown how the leaf anatomy of arctic plants responds to climate change.

We examined how elevated temperature and shading, applied in long-term field experiments in a subarctic and a high Arctic location, affect BVOC emission and leaf anatomy of the most dominant vascular plant species. The present study was conducted after 23 or 8 years of warming and shading treatments in the subarctic and the high Arctic location, respectively. We hypothesized that experimental warming would clearly increase the emissions from the individual plant shoots in a similar manner as observed at ecosystem level (Tiiva *et al*. 2008; Faubert *et al*. 2010), and that the leaves would get thinner in response to warming as commonly observed for trees (Higuchi *et al*. 1999; Luomala *et al*. 2005; Hartikainen *et al*. 2009, 2014). Shading was expected to decrease the emissions of the light-dependent BVOCs (Laothawornkitkul *et al*. 2009; Monson & Baldocchi 2014a) and lead to thinner leaves and reduced density of trichomes and stomata (Marques *et al*. 1999; Larcher 2003).

MATERIALS AND METHODS

Study site and experimental design

The study was conducted in the growing season of 2012 using three long-term field experimental set-ups with warming and shading treatments. One experiment was located in a heath in Abisko, Northern Sweden (68°21′ N, 18°49′ E), where the growing season usually extends from June to September. The climate is subarctic with a mean annual temperature and precipitation of 0.07 °C and 308 mm (1986–2006), respectively. The other two experiments were situated in a dry heath in Zackenberg, Northeast Greenland (71°30′ N, 20°30′ W). The climate is high Arctic with mean annual temperature of −7.9 °C (2003–2005), an average annual precipitation of 261 mm (1996–2005), and a growing season length of 2.0–3.5 months depending on year (Ellebjerg *et al*. 2008; Hansen *et al*. 2008). Air temperature and incoming photosynthetic photon flux density (PPFD over the waveband 400–700 nm) data for June to August 2012 at the two locations are presented in Fig. 1.

In all experiments, warming was achieved using dome-shaped open-top polyethylene film tents increasing air temperature by approximately 1 °C in Zackenberg (Ellebjerg *et al*. 2008) and 3–4 °C in Abisko (Havström *et al*. 1993). The shading was provided by dome-shaped hessian tents reducing the incoming PPFD by 50–60% (Ellebjerg *et al*. 2008; see

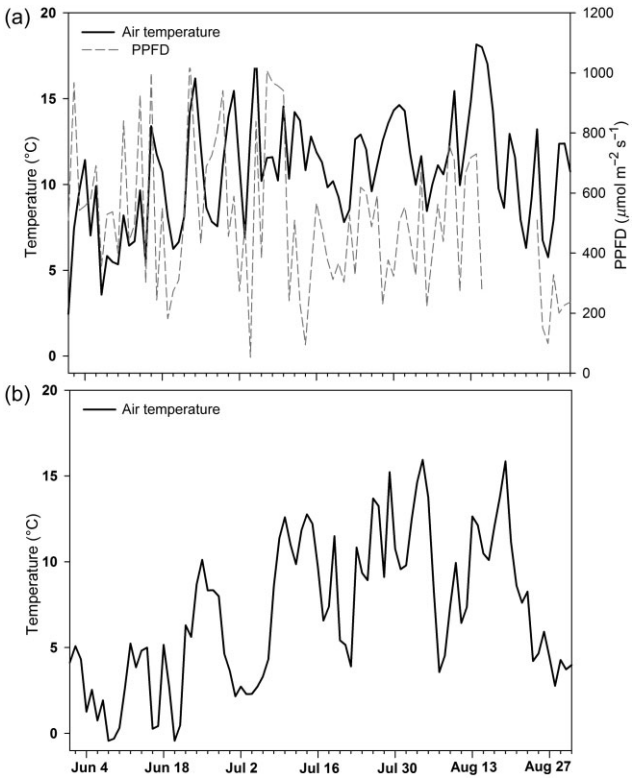


Figure 1. Mean daytime air temperature and photosynthetic photon flux density (PPFD) (2 m height, 0800–2000 h) in (a) Abisko and (b) Zackenberg during June to August 2012. No PPFD data was available for Zackenberg.

Table 1. Air temperature and PPFD during measurements

	Zackenberg		Abisko
	Cassiope tetragona	*Salix arctica*	
Air temperature (°C)			
July 3–4			16.4 ± 0.9
July 16/17	19.1 ± 1.2	19.5 ± 1.9	
July 30/31	26.5 ± 1.6	24.7 ± 0.8	
August 4–7			12.9 ± 0.3
August 13/14	19.4 ± 2.2	26.2 ± 1.3	
August 29		14.6 ± 1.3	
Effect of the shading treatment	–2.5	–4.5**	–0.8**
Effect of the warming treatment	1.4	–0.4	+4.4**
PPFD (μmol m^{-2} s^{-1})			
July 3–4			477 ± 29
July 16/17	1045 ± 125	738 ± 129	
July 30/31	1112 ± 33	1146 ± 86	
August 4–7			415.38 ± 7.74
August 13/14	599 ± 94	801 ± 102	
August 29		667 ± 53	
Effect of the shading treatment (%)	–68**	–56**	–63**
Effect of the warming treatment (%)	–12	–22*	–51**

Mean air temperature and incoming photosynthetic photon flux density (PPFD) in control treatment during measurements in each campaign and differences from control treatment in mean air temperature and PPFD during measurements in shading and warming treatments across campaigns. Decreases shown as negative values. Significant differences from the control are shown (Dunnett's test, $*P < 0.1$; $**P < 0.05$).

Table 1 for temperature and PPFD during the present study). Tents were set up each year for the snow-free period. Control plots were not covered with tents (Supporting Information Fig. S1).

In Abisko, the experiment has been maintained since 1989 (Havström *et al*. 1993). The treatments were arranged in six replicate blocks with control, warming and shading making up a total of 18 plots. In each of the two experiments in Zackenberg, established in 2004, the same treatments were replicated in five blocks (15 plots in each experiment). These experiments in Zackenberg only differed regarding vegetation cover: one was located in *Cassiope tetragona* (L.) D. Don-dominated heath and the other in *Salix arctica* Pall.-dominated heath.

Individual shoots of the dominant plant species were selected for the study. Plant shoots of each of the evergreen *Empetrum nigrum* ssp. *hermaphroditum* Hagerup and *C. tetragona* and the deciduous *Betula nana* L. were chosen in the Abisko experiment, whereas shoots of *C. tetragona* and the deciduous *S. arctica* were selected in the Zackenberg experiments (Supporting Information Fig. S2). Two measurement campaigns were conducted on July 3–4 and August 4–7 in Abisko. In Zackenberg, three measurement campaigns were done on July 17, July 31 and August 14 for *C. tetragona* and four were done on July 16, July 30, August 13 and August 29 for *S. arctica*.

Sampling and analysis of BVOC emissions

BVOC emissions from shoots of individual plant species were measured *in situ* by a dynamic enclosure system using polyethylene terephthalate (PET) bags (Rul-let Quality, Abena, Aabenraa, Denmark) as enclosures (Stewart-Jones & Poppy 2006). Flexible, disposable PET bags were convenient for collecting BVOCs from a large number of miniature-sized plants in remote field sites. The PET bags were pre-cleaned (120 °C, 60 min). Air was circulated through the PET bag of 1 L for 30 min by battery-operated pumps (12 V; Rietschle Thomas, Puchheim, Germany). The opening of the PET bag was tied around the stem together with the air inlet, while the air outlet was led through a hole in the bag. The incoming air with a flow of 500 mL min^{-1} was purified by a charcoal filter to remove particles and volatile contaminants present in the ambient air and by a MnO_2 scrubber to remove ozone (Ortega & Helmig 2008). BVOCs from the 6 L air sample, drawn through by 200 mL min^{-1}, were adsorbed in stainless steel cartridges (Markes International, Ltd., Llantrisant, UK) containing Tenax TA (150 mg) and Carbopack 1 TD (200 mg). The flow rates were calibrated using mini BUCK Calibrator M-5 and regulated using mass flow sensors (D6F-P0010A1, Omron, Kyoto, Japan). The cartridges were sealed with Teflon-coated brass caps until analysis. During the sampling, temperature and relative humidity inside the enclosure (DS1923, iButton Hygrochron temperature/humidity logger, Maxim integrated, San Jose, CA, USA) and PPFD (photosynthetic light smart sensor S-LIA-M003, connected to HOBO micro station data logger H21-002, Onset Computer Corporation, Boston, MA, USA) were recorded every minute and every tenth second, respectively. The enclosures led to a temperature increase of 1.7 ± 1.7 °C ($P = 0.3$, *t*-test) averaged across the campaigns in Abisko.

After all BVOC measurement campaigns, the plant shoots were harvested, air dried, and with the exception of *C. tetragona*, sorted into leaves and stems to measure dry mass and determine leaf area.

BVOCs were analysed by thermal desorber (UNITY2, Markes International, Ltd.) coupled to an ULTRA autosampler and gas chromatograph-mass spectrometer (7890A Series GC coupled with a 5975C inert MSD/DS Perfomance Turbo EI System, Agilent Technologies, Inc., Santa Clara, CA, USA). BVOCs were identified according to 26 standard compounds and by using the mass spectra in the NIST library. Subsequently, pure standards (Fluka, Buchs, Switzerland) in methanol were used for quantification in a following manner: isoprene for isoprene, α-pinene for monoterpenes (MTs), 1.8-cineole for oxygenated MTs (oMTs), α-humulene for sesquiterpenes (SQTs) and (E)-2-hexenal for other compounds. The standard solutions were injected into a stream of helium, which was directed through the cartridges and analysed as samples. The BVOCs not belonging to MTs, oMTs or SQTs were classified into other reactive volatile organic compounds (ORVOCs, having atmospheric lifetimes of <24 h, Guenther *et al*. 1995) or other volatile organic compounds (OVOCs).

Chromatograms were analysed using Enhanced ChemStation software (MSD ChemStation, E.02.01.1177, Agilent Technologies, Inc.) and information was extracted and sorted using an in-house function. Compounds that had an identification quality of the match with the NIST library above 90% were included in the dataset. Compounds originating from measurement or the analysis system were excluded. The excluded compounds were identified based on collection of volatile samples from empty PET bags.

The emission rate (E) was calculated according to: $E = [(C_{out} - C_{in}) \times F]/m_{dry}$, where C_{out} and C_{in} are the concentrations of BVOCs in the outlet and inlet air, F is the flow rate into the enclosure and m_{dry} is the leaf dry mass. Emissions per leaf area were additionally calculated for *B. nana* and *S. arctica*, for which, it was possible to accurately determine the leaf area. The concentration in the filtered inlet air was assumed to be zero (see Ortega & Helmig 2008; Niinemets *et al*. 2011).

Emissions of isoprene, MTs, oMTs and SQTs were standardized to 30 °C (Rinnan *et al*. 2014) and for isoprene to a PPFD of 1000 μmol m^{-2} s^{-1} using the algorithms presented by Guenther *et al*. (1993). This was done in order to estimate the emission potentials by excluding the momentary temperature effect during sampling and diurnal and daily variation. A β coefficient of 0.09 °C^{-1} was used for monoterpenes (Guenther *et al*. 1993) and 0.18 °C^{-1} for SQTs (Rinnan *et al*. 2011).

Leaf anatomy

Leaves were sampled when they were fully developed, but before the start of senescence. This was on July 6 in Abisko and on August 15 for *C. tetragona* and August 30 for *S. arctica* in Zackenberg. For the evergreen *E. hermaphroditum*, leaves from the previous growing season were used as the current year's leaves were not fully developed at the sampling time. All sampled leaves had developed during the long-term manipulations. The leaves of *E. hermaphroditum* are needle-like with margins curled downwards creating a cavity in the middle, where the stomata are found (Fig. 2a,c). On *C. tetragona* leaves, the margins are curled upwards creating an open cavity in the middle of the leaves making the leaves look deeply grooved (Fig. 2b,d). *S. arctica* and *B. nana* are both broadleaved with less complex leaves with adaxial (upper) palisade parenchyma layer and abaxial (lower) spongy parenchyma layer (Fig. 3).

Two leaves per species per plot were collected for light microscopy (LM) and immediately placed in 2.5% (v/v) glutaraldehyde fixative (in 0.1 M sodium cacodylate buffer). While in glutaraldehyde fixative, sections of about 1.5 × 1.5 mm were cut along the central midrib of *B. nana* and *S. arctica* leaves whereas 1.5 mm segments were cut from the middle part of *C. tetragona* and *E. hermaphroditum* leaves. Samples were stored in cold fixative until further processing.

Samples were rinsed in sodium cacodylate buffer (0.1 M), post-fixated with 1% osmium tetroxide (OsO_4) (in 0.1 M sodium cacodylate buffer), dehydrated with an ethanol series followed by a propylene oxide treatment, embedded in epon [Electron Microscopy Sciences, Hatfield, Pennsylvania, USA, Embed 812 (Zackenberg samples) and Ladd Research Industries, Williston, Vermont, USA, LX-112 (Abisko samples)]. 1.5 μm sections for LM were cut from the embedded samples using an ultramicrotome [Reichert-Jung Ultracut E, Wien, Austria, Diatomen histo-knife (Hi 4967)] and stained with toluidine blue and p-phenylene diamine (Kivimäenpää *et al*. 2010). LM sections were studied with a light microscope (Zeiss Primo Star light microscope, Jena, Germany and Olympus BX61 Automated upright microscope, Olympus Corporation, Tokyo, Japan) and photographed (Zeiss Axiocam ERc 5s camera, Jena, Germany and Olympus DP70 digital microscope camera, Tokyo, Japan). The objective magnification varied for the species. Digital images were analysed for thicknesses of the leaf, epidermis (including cuticle), and palisade and spongy parenchyma (Figs 2 & 3; Supporting Information Tables S 1 & S2). A shape change index was measured for *E. hermaphroditum* by dividing leaf cross section width by thickness (Fig. 2c). For *C. tetragona* and *E. hermaphroditum* the LM images were also used to calculate the numbers of trichomes and stomata per inner leaf surface length (Fig. 2c–f). In order to calculate the proportion of palisade and spongy parenchyma cells and intercellular space of the parenchyma, a grid was added to each image and the type of cell or intercellular space was recorded in each grid point.

Leaves for scanning electron microscopy (SEM) analysis were air dried, cut to pieces that fitted to be mounted on aluminium stubs and coated with gold-platinum (~50 nm) under vacuum (Automatic Sputter Coater B7341, Agar Scientific, Ltd., Stansted, UK). The samples were examined using SEM (Philips XL30 ESEM-TMP, FEI Company, Eindhoven, the Netherlands) and digitally photographed at ×300–700 magnification depending on species and surface structure to be examined. Digital images of surface structures were analysed for trichome and stomatal density. All analyses of

© 2015 The Authors.

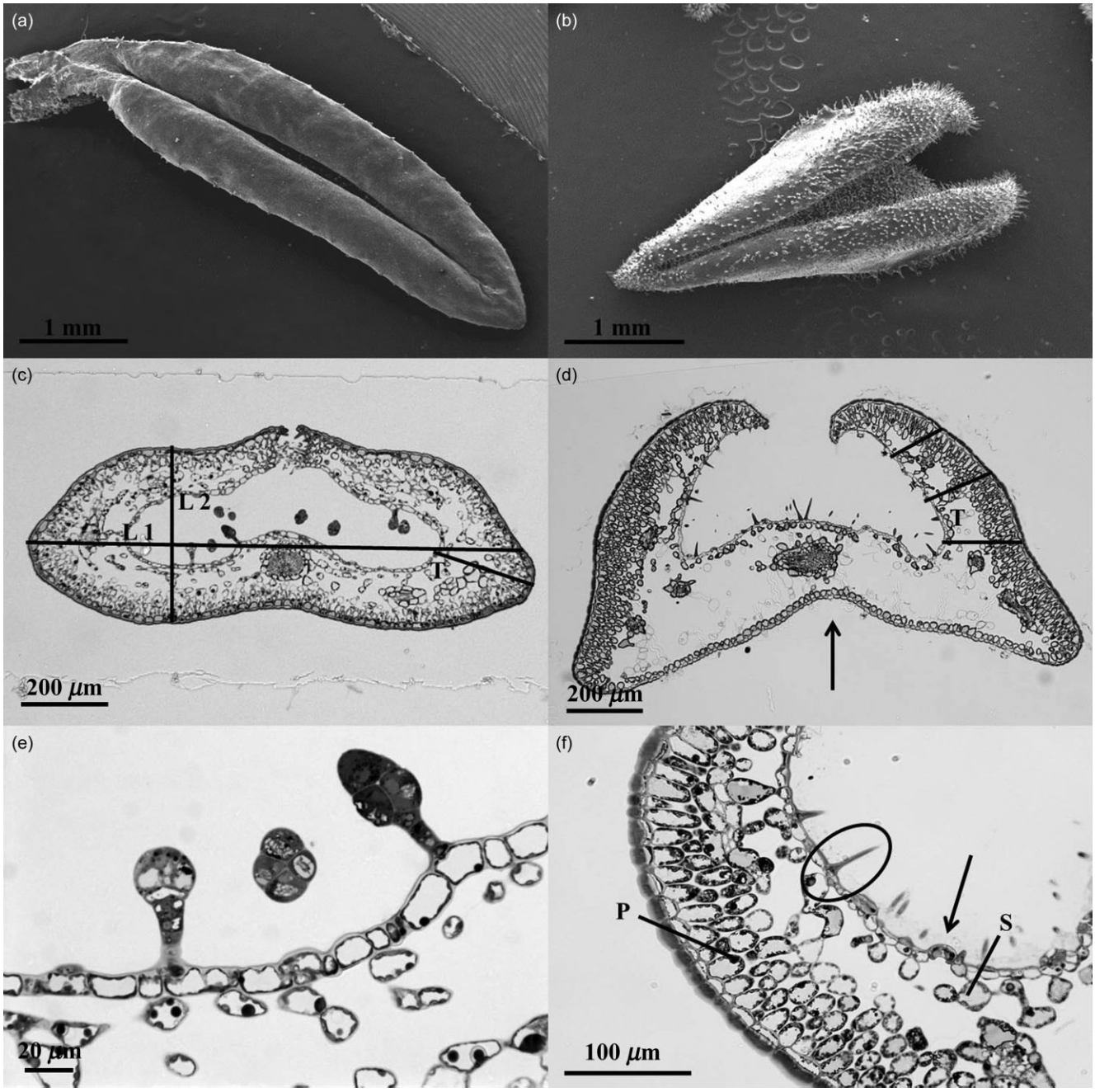


Figure 2. Scanning electron microscopy (SEM) images of (a) *Empetrum hermaphroditum* and (b) *Cassiope tetragona* leaves, where spiky, non-glandular trichomes appear on the surface. Light microscopy (LM) images of cross section for (c) *E. hermaphroditum* and (d) *C. tetragona* show the inner cavity within the leaves of the two species created by the curled margins. The cavity of *C. tetragona* faces directly away from the stem (arrow points at the surface against stem), whereas the one of *E. hermaphroditum* faces downwards. (e) glandular trichomes on the inner surface of *E. hermaphroditum* and (f) stoma (arrow) and spiky trichome (circle) on the inner surface of *C. tetragona*. Palisade (P) and spongy (S) parenchyma are marked. Glandular trichomes also occurred on the inner surface of *C. tetragona* and on the surface facing the stem, particularly for *C. tetragona* collected in Abisko. For *E. hermaphroditum*, the shape change index was measured as the ratio between length 1 (L1) and 2 (L2) and leaf thickness (T) was measured at the thickest point where the leaf curls. For *C. tetragona*, T was estimated as an average of three points. Thicknesses of other tissues were measured at the same point as T for both species.

digital images were done using ImageJ (1.47 v, Wayne Rasband, National Institutes of Health, Bethesda, Maryland, USA).

Leaf dry mass per area (M_A) was measured for the broadleaved *B. nana* and. *S. arctica*.

Data analysis

Statistical analyses were conducted using SAS 9.4 (SAS Institute Inc., Cary, NC, USA). Treatment effects on BVOC emissions across the study period were tested by repeated

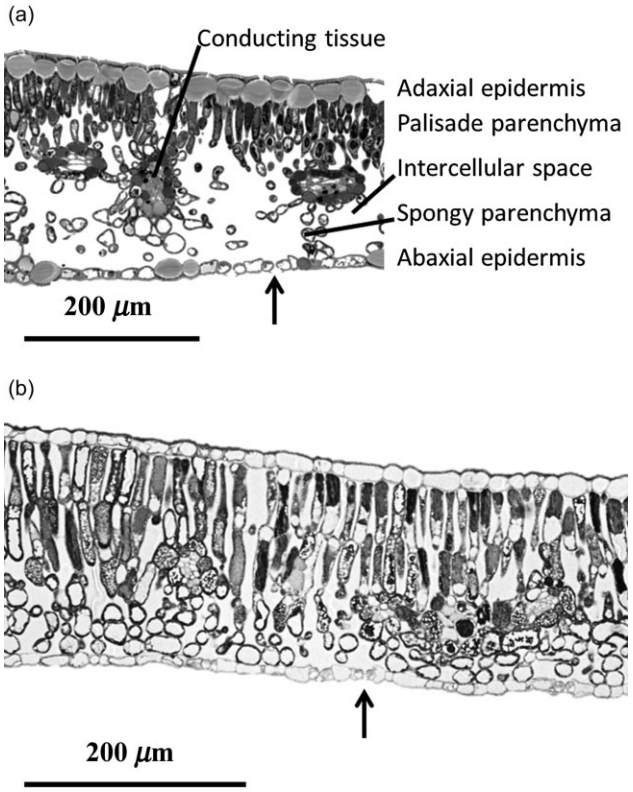


Figure 3. Light microscopy (LM) images of cross section of (a) *B. nana* and (b) *S. arctica*. Stomata (arrows) are visible on the abaxial surface.

measures linear mixed model. Treatment and time (and their interaction) were included as fixed factors, whereas block was used as a random factor. However, time and the interaction term were excluded from the model when $P \geq 0.2$. Furthermore, the block factor was excluded from the model when background variation could not be assigned to the differences between blocks, that is when the covariance parameter estimate was ≤0. Repeated factor was set to a number of campaign and subject to plot. Selection of covariance structure was based on the smallest Akaike's information criteria (AIC) and was set to either compound symmetry (CS), Autoregressive [Ar(1)] or Toeplitz (TOEP).

Analysis of variance was used to assess the treatment effects on BVOC emissions within each campaign with treatment and block as factors. Block was excluded when $P \geq 0.2$. Dunnett's test was used to compare the warming and shading treatment to the control. Similar models were also used to assess treatment effects on anatomy variables. As comparison of species was not the purpose of this study, each species was subjected to separate analyses. Transformations were made when the variances were heterogenic.

Partial least squares regression (PLS) was used to test whether the common leaf anatomy data for the broadleaved species *B. nana* and *S. arctica* correlates with the BVOC emission data using SIMCA (Umetrics, version 13.0.3.0, Umeå, Sweden). The emission data used for the PLS originated from the campaign with highest BVOC emissions. The data from July 3 to 4 was therefore chosen for *B. nana* and those from July 30 for *S. arctica*. PLS components were extracted following centring and unit variance scaling of the variables, and the PLS model was evaluated by segmented cross validation using six segments based on the maximum number of blocks in the experiments. The scores for the two first PLS components were analysed by similar models as described earlier.

RESULTS

Treatment effects on BVOC emissions

Abisko

For *E. hermaphroditum*, no significant treatment effects were found for emission or emission potential of any of the compound groups (Supporting Information Tables S3a & S5a). ORVOCs, with 3-hexenol and 3-hexenal as the major compounds, constituted 47% of the total emissions averaged across campaigns (Fig. 4a). Isoprene constituted 26% of the total emissions averaged across campaigns, and MT and SQT minor part of the emissions with 1 and 12%, respectively.

There were no statistically significant treatment effects on emissions or emission potentials of *C. tetragona* (Supporting Information Tables S3b & S5a). However, shading tended to increase the oMT and MT emission potentials within the August 4–7 campaign ($P < 0.1$, Dunnett's test) (Supporting Information Table S5a). MTs and oMTs constituted 11 and 4% of the total measured emissions averaged across campaigns with limonene and cymene being the most emitted MTs, and eucalyptol and α-terpineol the most emitted oMTs. ORVOCs, with butyl benzoate and 2,2,4-trimethyl-1,2-dihydroquinoline as the dominant compounds, represented the largest proportion (31%) of the averaged total BVOC emission (Fig. 4b). *C. tetragona* emitted a notable amount of isoprene especially in the August 4–7 campaign, where the emission averaged for the treatments was 1.5 μg g^{-1} h^{-1}. The total SQT emission constituted 16% of the total mean BVOC emission.

For *B. nana*, treatment effects were only found in the July 3–4 campaign, where warming led to a significantly decreased emission of isoprene, OVOCs and total BVOCs ($P < 0.05$, Dunnett's test) (Supporting Information Table S3c). Shading significantly decreased the isoprene and OVOC emission, while increasing the SQT emission on July 3–4. Emission potentials showed similar effects for isoprene and SQTs (Supporting Information Table S5a). ORVOCs, which constituted 79% of the total emission averaged across campaigns, were not affected by the treatments (Fig. 4c). The dominant compounds in this group were 3-hexenol and 3-hexenyl butyrate. The dry mass- and leaf area-based emissions showed consistent results (data not shown).

Zackenberg

S. arctica only showed a significant treatment effect on July 30 when isoprene emission and emission potential were significantly reduced by the shading (Supporting Information Tables S4a & S5b). Additionally, shading led to a tendency

© 2015 The Authors. *Plant, Cell & Environment* published by John Wiley & Sons Ltd,

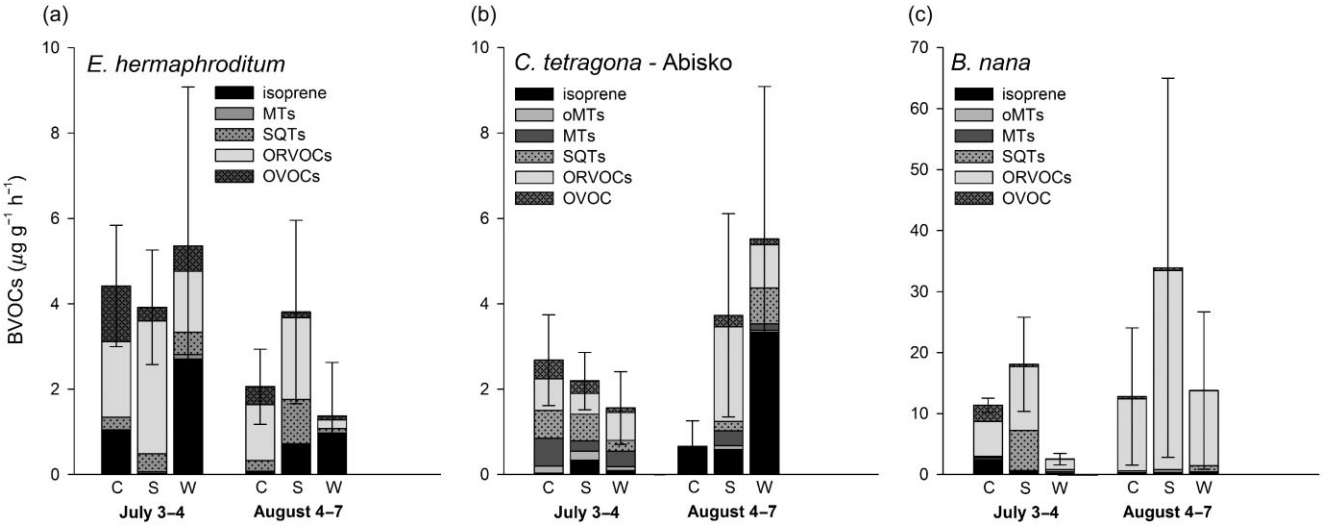


Figure 4. Mean BVOC emissions (±SE for totals; $n = 4–6$) for (a) *Empetrum hermaphroditum*, (b) *Cassiope tetragona* and (c) *Betula nana* in control (C), shading (S) and warming (W) treatments in Abisko during two measurement campaigns in the growing season. Contributions of isoprene, oxygenated monoterpenes (oMTs) non-oxygenated monoterpenes (MTs), sesquiterpenes (SQTs), other reactive volatile organic compounds (ORVOCs) and other volatile organic compounds (OVOCs) to the total BVOC emission are shown. Significant treatment effects were only found for *B. nana* (see Supporting Information Table S3a, b and c for statistics). Note the different *y*-axis scales.

towards a decrease in the measured OVOC emission on July 16. The *S. arctica* emission was dominated by ORVOCs (Fig. 5a), which represented 60% of the emissions and had 2-hexenyl acetate and 2-hexenal as dominant compounds. The most emitted single compound, isoprene, constituted 38% of the total mean BVOC emission. Isoprene emission was particularly high on July 30 where the emission rate averaged for the treatments was 8.53 μg g^{-1} h^{-1}. Also for *S. arctica*, the dry mass- and leaf area-based emissions showed consistent results (data not shown).

No significant treatment effects were found for emissions or emission potentials of *C. tetragona* (Supporting Information Tables S4b & S5b). A tendency towards an increased SQTs emission was found on July 17 because of warming (Supporting Information Table S4b). ORVOCs constituted 52% of the total BVOC emission averaged across the

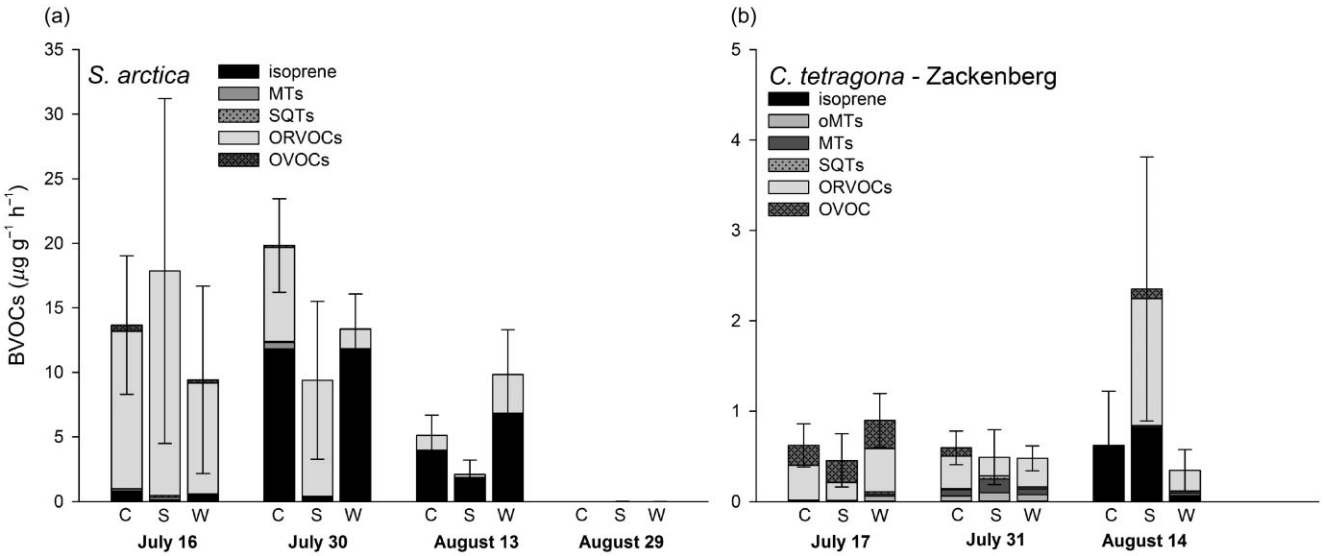


Figure 5. Mean BVOC emissions (±SE for totals; $n = 3–5$) for (a) *Salix arctica* and (b) *Cassiope tetragona* in control (C), shading (S) and warming (W) treatments in Zackenberg during four and three measurement campaigns, respectively, in the growing season. Contributions of isoprene, oxygated monoterpenes (oMTs) non-oxygenated monoterpenes (MTs), sesquiterpenes (SQTs), other reactive volatile organic compounds (ORVOCs) and other volatile organic compounds (OVOCs) to the total BVOC emission are shown. Significant treatment effects were only found for *S. arctica* (see Supporting Information Table S4a and b for statistics). Note the different *y*-axis scales.

© 2015 The Authors. *Plant, Cell & Environment* published by John Wiley & Sons Ltd,

campaigns (Fig. 5b), and had benzaldehyde, hexane and methylcyclopentane as the major compounds. Isoprene was detected with noteworthy emissions on August 14, when a mean emission for all treatments was 0.5 $\mu g\ g^{-1}\ h^{-1}$. Total MT emission represented 10% of the mean total BVOC emission, whereas SQTs constituted 2%.

Lists of individual compounds detected for each species are shown in Supporting Information Table S6 and S7.

Treatment effects on leaf anatomy

Abisko

While warming had no significant effects on the leaf anatomy of *E. hermaphroditum*, shading altered it by making the needle-like curled leaves broader, but flatter (significantly higher shape change index in Table 2). The leaf thickness was also significantly increased by shading. Furthermore, shading significantly decreased the stomatal density and tended to decrease the spongy parenchyma thickness (Table 2).

For *C. tetragona*, warming significantly increased the thickness of the inner epidermis (towards the cavity) and had a tendency to decrease palisade : spongy parenchyma ratio (Table 2). Warming also had a tendency to decrease the density of glandular trichomes on the inner surface, while leading to a significant increase in the stomatal density (Table 2). Shading significantly increased the stomatal density, decreased the thickness of the outer epidermis (facing outwards), and tended to cause fewer trichomes on the surface facing the stem.

For *B. nana*, warming increased the leaf thickness by 13%, and this increase was nearly significant (Table 2). Warming also caused a significantly thicker spongy parenchyma and a decreased palisade : spongy parenchyma ratio (Table 2). Shading significantly decreased this ratio, and the thickness of the palisade parenchyma.

Zackenberg

Warming significantly increased the thickness of the adaxial epidermis and decreased the palisade : spongy parenchyma ratio for *S. arctica* (Table 2).

Neither warming nor shading had statistically significant effects on the leaf anatomy of *C. tetragona* from Zackenberg. However, a not statistically significant increase in the thickness of the inner epidermis and a decrease in the palisade : spongy parenchyma ratio under warming was similar to the significant alterations found for *C. tetragona* from Abisko (Table 2 & Supporting Information Table S2b).

Covariance between leaf anatomy and BVOC emissions

The PLS regression was used to test if leaf anatomy (*x* variables) could explain some variation in the BVOC emissions

Table 2. Leaf anatomy variables of *Empetrum hermaphroditum*, *Cassiope tetragona*, *Betula nana* from Abisko and *Salix arctica* and *C. tetragona* from Zackenberg

	Control	Shading	Warming
Abisko			
E. hermaphroditum			
Shape change index[a]	2.5 ± 0.0	2.9 ± 0.1 ↑**	2.6 ± 0.1
Leaf thickness (μm)	265.2 ± 7.1	301.4 ± 6.8 ↑**	289.9 ± 13.6
Spongy parenchyma thickness (μm)	77.5 ± 4.2	65.6 ± 3.8 ↓*	81.2 ± 3.6
Stomatal density on inner surface (#/mm)	3.4 ± 0.4	1.8 ± 0.2 ↓**	3.2 ± 0.5
C. tetragona			
Outer epidermis thickness (μm)	21.8 ± 0.7	17.7 ± 0.9 ↓**	21.6 ± 0.9
Inner epidermis thickness (μm)	10.1 ± 0.4	9.9 ± 0.2	11.9 ± 0.4 ↑**
Palisade : spongy parenchyma ratio	0.9 ± 0.1	0.9 ± 0.0	0.8 ± 0.1 ↓*
Glandular trichomes on inner surface (#/mm)	1.2 ± 0.1	1.2 ± 0.3	0.5 ± 0.2 ↓*
Total trichomes on surface against stem (#/mm)	5.8 ± 0.7	4.5 ± 0.9 ↓*	5.9 ± 0.5
Stomatal density on inner surface (#/mm)	2.0 ± 0.2	3.3 ± 0.7 ↑**	3.3 ± 0.4 ↑**
B. nana			
Leaf thickness (μm)	206.3 ± 5.7	193.2 ± 6.3	233.5 ± 13.0 ↑*
Palisade parenchyma thickness (μm)	70.6 ± 1.9	48.7 ± 3.3 ↓**	76.3 ± 5.1
Spongy parenchyma thickness (μm)	94.4 ± 3.0	102.1 ± 2.1	119.4 ± 8.5 ↑**
Palisade : spongy parenchyma ratio	0.8 ± 0.0	0.5 ± 0.0 ↓**	0.6 ± 0.0 ↓**
Zackenberg			
S. arctica			
Adaxial (upper) epidermis thickness (μm)	17.1 ± 1.0	18.6 ± 0.9	21.1 ± 1.1 ↑**
Palisade : spongy parenchyma ratio	1.6 ± 0.1	1.2 ± 0.1	1.1 ± 0.1 ↓**
C. tetragona			
No significant effects of shading or warming			

[a]Measured by dividing leaf cross section width by thickness (see Fig. 2c).
Only variables with significant effects of warming or shading are shown (Dunnett's test, $*P < 0.1$; $**P < 0.05$). Values are means (±SE; $n = 5–6$). Arrows indicate a decrease or increase compared with the control treatment.

© 2015 The Authors. *Plant, Cell & Environment* published by John Wiley & Sons Ltd,

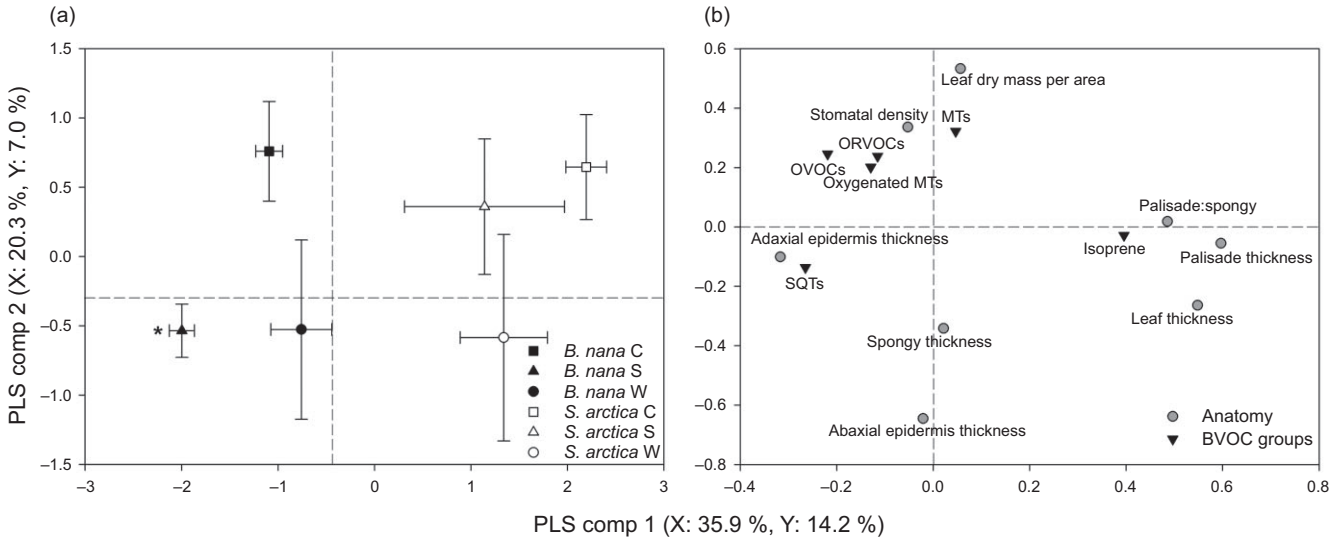


Figure 6. Partial least squares (PLS) regression showing the relationship between leaf anatomy variables common for *Betula nana* and *Salix arctica* and the unstandardized emissions of BVOCs divided into isoprene, oxygenated monoterpenes (oMTs), non-oxygenated monoterpenes (MTs), sesquiterpenes (SQTs), other reactive volatile organic compounds (ORVOCs) and other volatile organic compounds (OVOCs). (a) The mean scores (±SE; $n = 3$–6) for the control (C), shading (S) and warming (W) treatments of the components (PLS comp 1 and PLS comp 2) and (b) the corresponding loading variables. The explained variances of the independent (x) and dependent (y) data are shown in parentheses. Treatments within species having significant different mean than the control along the respective PLS comp are shown (Dunnett's test, $*P < 0.05$).

(y variables) in the broadleaved *S. arctica* and *B. nana*. The PLS component 1 showed a clear separation between the species ($P < 0.01$), and explained 36% of the variation in the x variables and 14% of the variation in the y variables (Fig. 6a). For *B. nana*, the shading treatment was clearly different from the control ($P < 0.05$, Dunnett's test). The PLS component 2 explained 20% of the variation in the x variables and 7% of the variation in the y variables.

The regression coefficients revealed a positive correlation between isoprene emission, and the leaf anatomy variables palisade : spongy parenchyma ratio, leaf thickness and palisade parenchyma thickness (Figs 6b & 7). Furthermore, isoprene emission had a significant negative correlation with adaxial epidermis thickness (Figs 6b & 7). Isoprene emission did not correlate with abaxial epidermis, spongy parenchyma thickness, stomatal density or leaf dry mass per area. No significant correlations were found between leaf anatomy variables and oMTs, MTs or ORVOCs, respectively (Supporting Information Fig. S3a,b,d). SQT emission showed a significant negative correlation with palisade : spongy parenchyma ratio (Supporting Information Fig. S3c). The emission of OVOCs correlated negatively with the palisade : spongy parenchyma ratio and the palisade parenchyma thickness (Supporting Information Fig. S3e).

DISCUSSION

We expected to find increased BVOC emissions because of warming as observed at the ecosystem level in the Subarctic (Tiiva *et al*. 2008; Faubert *et al*. 2010) and in the majority of studies applying experimental warming (Peñuelas & Staudt 2010). Shading was expected to reduce BVOC emissions due to the light-dependency of many BVOCs (Laothawornkitkul *et al*. 2009; Monson & Baldocchi 2014a). However, BVOC emissions from the studied arctic plant species were barely

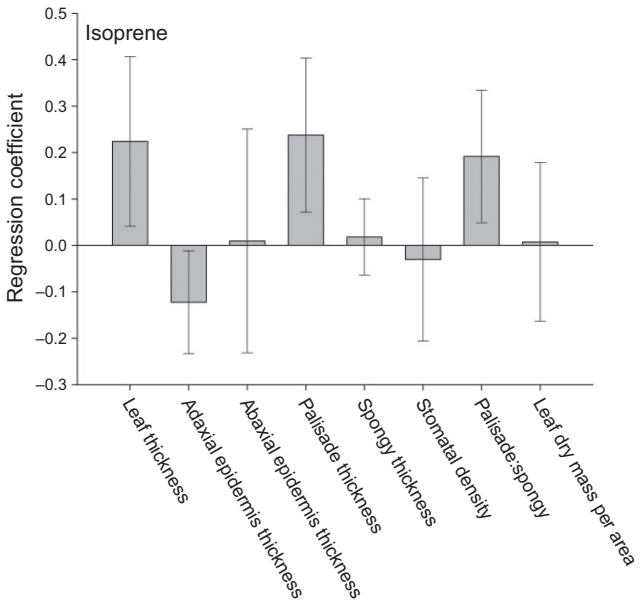


Figure 7. Regression coefficients of a partial least squares (PLS) model for the various leaf anatomy variables affecting isoprene emission. Error bars indicate ± 2 standard deviations of the regression coefficients. When the error bar does not include zero, the variable has a significant contribution in explaining the isoprene emission rate.

affected by warming and shading. This was an unexpected result, which is in accordance with previous findings from the arctic region (Rinnan *et al*. 2011). Whereas Rinnan *et al*. (2011) could offer no mechanistic explanation for the lack of effects, we suggest that it may be partly explained by long-term acclimation of the plants to the mimicked climate change, as shown by the anatomy responses. Furthermore, low emission rates combined with high natural variation may have reduced the potential of detecting differences.

Our results suggest that anatomy responses of arctic plants to warming differ from species from lower latitudes, whereas the effects of shading were more comparable with earlier studies (Larcher 2003). Most boreal forest species have responded to long-term warming in field exposures by modifying leaf structure towards for example thinner leaves and epidermis, and lower density of stomata. In an open-field experiment, Hartikainen *et al*. (2009, 2014) found thinner leaves and epidermis of *P. tremula* and thinner epidermis of *Betula pendula* when exposed to infrared heaters, while Luomala *et al*. (2005) observed thinner needles in *Pinus sylvestris* in response to warming by closed-top enclosures of individual trees. Luomala *et al*. (2005) also reported decreased stomatal density in *P. sylvestris*. In contrast to these boreal species, we found warming to result in thicker leaves of *B. nana* and thicker epidermis for both *C. tetragona* and *S. arctica* indicating prevention of water loss (Larcher 2003) and increased stomatal density in *C. tetragona* in Abisko. In the studies of Hartikainen *et al*. (2009, 2012), *P. tremula* and *B. pendula* were additionally found to emit significantly more BVOCs under warming, which is also opposite from our results.

In accordance with Hartikainen *et al*. (2009), we found that leaf anatomy variables for the studied broadleaved species explained some variation in BVOC emissions. By a PLS regression we showed that isoprene emission increased with increasing thickness of the leaf and palisade parenchyma, increasing palisade : spongy parenchyma ratio and decreasing epidermis thickness. Isoprene is formed in the chloroplasts of the parenchyma and the emission is strongly bound to photosynthetic carbon metabolism (Loreto & Schnitzler 2010; Li & Sharkey 2013). As the tightly packed palisade parenchyma beneath the top epidermis has a high potential for photosynthesis (Monson & Baldocchi 2014b), a leaf with thinner palisade parenchyma might offer less sites for photosynthesis and BVOC synthesis (Hartikainen *et al*. 2009) leading to lower isoprene emission. The observed lower palisade : spongy parenchyma ratio could thus partly explain why warming did not increase isoprene emission in *S. arctica*. The production of other isoprenoids synthesized in the palisade cells (Loreto & Schnitzler 2010; Li & Sharkey 2013) could likewise be affected by a decrease in the palisade : spongy parenchyma ratio, also observed for *B. nana* and *C. tetragona*. Also, acclimation of BVOC synthesis because of decrease in gene transcription and enzyme activities could be a potential explanation for the unaltered emissions. However, molecular biological analyses were not feasible in this field-based study.

Thinner leaves might also have less BVOC synthetizing tissue per unit leaf area, and isoprene emission did positively correlate with leaf thickness. However, as opposed to other studies (e.g. Larcher 2003; Luomala *et al*. 2005; Hartikainen *et al*. 2009; Rasulov *et al*. 2014), we found that warming increased leaf thickness in *B. nana* and shading in *E. hermaphroditum*. In their study, Hartikainen *et al*. (2009) reasoned that warming-induced thinner leaves promoted BVOC emissions from *P. tremula* due to shorter diffusion pathways for BVOCs to exit the leaves. A greater thickness would on the other hand result in longer diffusion pathways (cf. Noe *et al*. 2008; Hartikainen *et al*. 2009), increased residence time of BVOCs inside the leaf and thereby enhanced probability of within-leaf metabolism (Niinemets *et al*. 2014) and reduced net emissions. New evidence suggests a reactive diffusion pathway, where a large proportion of isoprenoids can be oxidized along the pathway from site of synthesis to the atmosphere, whereby the emission does not equal the production (especially under oxidative stress Jardine *et al*. 2013; Niinemets *et al*. 2014).

The epidermis thickness has been suggested to influence the diffusion of lipophilic BVOCs across the epidermis (Hartikainen *et al*. 2009). Our observation of a negative correlation between the adaxial epidermis thickness and isoprene emission supports this hypothesis. A thicker adaxial/inner epidermis in *S. arctica* and *C. tetragona* in response to warming may be a structural adaptation to avoid increased transpiration under warming and at the same time constrain BVOC emissions. Except for stored BVOCs in for example trichomes, BVOCs however, almost entirely escape through stomata when these are open (Harley 2013; Niinemets *et al*. 2014). Stomatal conductance can exert short-term control on the BVOC emission until a steady state is resumed (Niinemets *et al*. 2004; Harley 2013). However, our PLS results showed no correlation between BVOC emissions and stomatal density, and thus support the idea that stomata cannot control emissions over long term (Niinemets & Reichstein 2003). The changes we observed in stomatal density – a decrease under shading in *E. hermaphroditum* and an increase due to both warming and shading in *C. tetragona* in Abisko – are thus unlikely to affect BVOC emissions.

BVOCs stored in surface structures, for example many MTs, escape directly to the atmosphere depending on the temperature-dependent volatilization from storage pools (Laothawornkitkul *et al*. 2009). Warming decreased the density of glandular trichomes for *C. tetragona* in Abisko, whereas MT emissions were not affected. Less trichomes could reduce emission of stored BVOCs from this strong MT emitter (Rinnan *et al*. 2011; Schollert *et al*. 2014) and thus limit the expected increased emission under warming.

E. hermaphroditum was the only studied species, which showed neither leaf anatomy nor emission responses to elevated temperature. This lack of responses may be explained by the wide circumpolar and -boreal distribution of the *Empetrum* spp. in the northern hemisphere as far south as 40° N (Popp *et al*. 2011). The subspecies *E. hermaphroditum* might thus be able to thrive at higher

temperatures than simulated by this experiment and have no need for structural acclimation. The anatomy responses of *E. hermaphroditum* to shading, on the contrary, indicate a greater sensitivity towards decreased amount of light. In general, the responses to shading in all the species studied here were similar to typical acclimations to shady habitats (Larcher 2003) with increased leaf thickness in *E. hermaphroditum* and increased stomatal density of *C. tetragona* in Abisko being exceptions.

C. tetragona showed no significant emission responses to the treatments at either of the two locations. The anatomy responses were, however, similar: the inner epidermis thickness increased and palisade : spongy parenchyma ratio decreased because of warming at both locations, but statistically significantly only in Abisko. There are three potential explanations to stronger anatomical alterations in Abisko: (1) *C. tetragona* may be more sensitive to temperature changes near its southern limit, Abisko (Weijers *et al*. 2012), while the species might benefit from warming in the high arctic Zackenberg; (2) The species had a longer time to respond in Abisko as the experiment had been running 15 more years than in Zackenberg and as the growing season is longer; and (3) The temperature impact of open-top chambers (OTCs) differs widely across sites (Bokhorst *et al*. 2013) and here the greater temperature increase in the warming treatment in Abisko might be partly responsible for the greater anatomy responses.

In Abisko, the open-top tents used in the warming treatment reduced the PPFD level during the measurements by 51%. Even though summer warming by OTCs is strongly coupled with the solar irradiance (Bokhorst *et al*. 2013), a >4 °C temperature increase still occurred. The reduced PPFD level could have limited the warming effect because of the light-dependency of many BVOCs (Laothawornkitkul *et al*. 2009; Monson & Baldocchi 2014a). Nevertheless, the ecosystem-level BVOC emissions have drastically increased under warming by similar tents in another experiment in Abisko (Tiiva *et al*. 2008; Faubert *et al*. 2010), and significant changes in vegetation and soil indicating long-term warming have been reported (Michelsen *et al*. 2012). In contrast to Abisko, the OTCs in Zackenberg caused no or only a slight temperature increase and at most a 22% decrease in the PPFD level. As earlier measurements report a 1 °C increase in the warming treatment (Ellebjerg *et al*. 2008; Campioli *et al*. 2013), we expect this to be the general pattern. Most studies using OTCs and greenhouses acknowledge the potentially confounding effects on the enclosed microclimate, which can differ in intensity and direction for different sites (Bokhorst *et al*. 2013). Confounding effects such as decreased soil moisture, PPFD level and wind speeds are well-known (Havström *et al*. 1993; Bret-Harte *et al*. 2001; Bokhorst *et al*. 2013). The confounding temperature decrease in the shading treatment in this study might have affected the BVOC emissions negatively especially in Zackenberg, where the decrease was most profound. It should, thus, be kept in mind that the measured emissions only give a snapshot at a point in time, whereas the observed alterations in leaf anatomy reflect long-term effects of the treatments.

Climate change is expected to radically increase the plant biomass and alter vegetation composition in the arctic region (Walker *et al*. 2006; Elmendorf *et al*. 2012; Michelsen *et al*. 2012). These changes will likely lead to changes in the quantity and quality of BVOC emissions (see Rinnan *et al*. 2014). Thus, even if warming does not increase the emissions at plant shoot-level, which may partly be due to anatomical acclimation, the ecosystem-level emissions are nevertheless expected to increase as the plant cover and biomass will be higher.

ACKNOWLEDGMENTS

This work was funded by the Villum Foundation, the Danish Council for Independent Research|Natural Sciences and the Maj and Tor Nessling Foundation. We wish to thank the Abisko Scientific Research Station and the Zackenberg Research Station for excellent facilities and logistical support. We thank Abisko Scientific Research Station and Asiaq, Greenland Survey, for providing climate data. Furthermore, we would like to thank the personal of the BIOBASIS programme for maintenance of the experiments in Zackenberg and Anders Michelsen for maintenance of the experiment in Abisko. We are grateful for assistance and company in the field by Tora F. Nielsen and Jacqueline M. Anderson and for technical assistance by Virpi Miettinen (SIB-labs, University of Eastern Finland), Gosha Sylvester, Esben V. Nielsen (Department of Biology, University of Copenhagen), Timo Oksanen, Helena Ruhanen and Virpi Tiihonen (Department of Environmental Science, University of Eastern Finland). We also thank the Danish National Research Foundation for supporting activities within the Center for Permafrost (CENPERM DNRF100), University of Copenhagen.

REFERENCES

Arneth A., Harrison S.P., Zaehle S., Tsigaridis K., Menon S., Bartlein P.J., . . . Vesala T. (2010) Terrestrial biogeochemical feedbacks in the climate system. *Nature Geoscience* **3,** 525–532.

Beerling D.J. & Chaloner W.G. (1993) The impact of atmospheric CO_2 and temperature change on stomatal density: observations from *Quercus robur* Lammes leaves. *Annals of Botany* **71,** 231–235.

Bokhorst S., Huiskes A., Aerts R., Convey P., Cooper E.J., Dalen L., . . . Dorrepaal E. (2013) Variable temperature effects of open top chambers at polar and alpine sites explained by irradiance and snow depth. *Global Change Biology* **19,** 64–74.

Bret-Harte M.S., Shaver G.R., Zoerner J.P., Johnstone J.F., Wagner J.L., Chavez A.S., . . . Laundre A. (2001) Developmental plasticity allows *Betula nana* to dominate tundra subjected to an altered environment. *Ecology* **82,** 18–32.

Campioli M., Schmidt N.M., Albert K.R., Leblans N., Ro-Poulsen H. & Michelsen A. (2013) Does warming affect growth rate and biomass production of shrubs in the high Arctic? *Plant Ecology* **214,** 1049–1058.

Ellebjerg S.M., Tamstorf M.P., Illeris L., Michelsen A. & Hansen B.U. (2008) Inter-annual variability and controls of plant phenology and productivity at Zackenberg. In *Advances in Ecological Research* (eds H. Meltofte, T.R. Christensen, B. Elberling, M.C. Forchhammer & M. Rasch), pp. 249–273. Academic Press, London, UK.

Elmendorf S.C., Henry G.H.R., Hollister R.D., Björk R.G., Bjorkman A.D., Callaghan T.V., . . . Wookey P.A. (2012) Global assessment of experimental climate warming on tundra vegetation: heterogeneity over space and time. *Ecology Letters* **15,** 164–175.

Faubert P., Tiiva P., Rinnan Å., Michelsen A., Holopainen J.K. & Rinnan R. (2010) Doubled volatile organic compound emissions from subarctic tundra under simulated climate warming. *The New Phytologist* **187,** 199–208.

Fineschi S., Loreto F., Staudt M. & Peñuelas J. (2013) Diversification of volatile isoprenoid emissions from trees: evolutionary and ecological perspectives. In *Biology, Controls and Models of Tree Volatile Organic Compound Emissions* (eds Ü. Niinemets & R.K. Monson), pp. 1–20. Springer, Berlin.

Grote R., Monson R.K. & Niinemets Ü. (2013) Leaf-level models of constitutive and stress-driven volatile organic compound emissions. In *Biology, Controls and Models of Tree Volatile Organic Compound Emissions* (eds Ü. Niinemets & R.K. Monson), pp. 315–355. Springer, Berlin.

Guenther A., Hewitt C.N., Erickson D., Fall R., Geron C., Graedel T., . . . Zimmerman P.R. (1995) A global model of natural volatile organic compound emissions. *Journal of Geophysical Research. Atmospheres: JGR* **100,** 8873–8892.

Guenther A.B., Zimmerman P.R., Harley P.C., Monson R.K. & Fall R. (1993) Isoprene and monoterpene emission rate variability: model evaluations and sensitivity analyses. *Journal of Geophysical Research* **98,** 12609–12617.

Hansen B.U., Sigsgaard C., Rasmussen L., Cappelen J., Hinkler J., Mernild S.H., . . . Hasholt B. (2008) Present-day climate at Zackenberg. In *Advances in Ecological Research* (eds H. Meltofte, T.R. Christensen, B. Elberling, M.C. Forchhammer & M. Rasch), pp. 111–149. Academic Press, London, UK.

Harley P.C. (2013) The roles of stomatal conductance and compound volatility in controlling the emission of volatile organic compounds from leaves. In *Biology, Controls and Models of Tree Volatile Organic Compound Emissions* (eds Ü. Niinemets & R.K. Monson), pp. 181–208. Springer, Berlin.

Hartikainen K., Nerg A.-M., Kivimaenpaa M., Kontunen-Soppela S., Maenpaa M., Oksanen E., . . . Holopainen T. (2009) Emissions of volatile organic compounds and leaf structural characteristics of European aspen (*Populus tremula*) grown under elevated ozone and temperature. *Tree Physiology* **29,** 1163–1173.

Hartikainen K., Riikonen J., Nerg A.-M., Kivimäenpää M., Ahonen V., Tervahauta A., . . . Holopainen T. (2012) Impact of elevated temperature and ozone on the emission of volatile organic compounds and gas exchange of silver birch (*Betula pendula* Roth). *Environmental and Experimental Botany* **84,** 33–43.

Hartikainen K., Kivimäenpää M., Nerg A.-M., Mäenpää M., Oksanen E., Rousi M. & Holopainen T. (2014) Elevated temperature and ozone modify structural characteristics of silver birch (Betula pendula) leaves. In *Effects of elevated temperature and/or ozone on leaf structural characteristics and volatile organic compound emissions of northern deciduous tree and crop species*, pp. 81–116. PhD thesis, Publications of the University of Eastern Finland, Dissertations in Forest and Natural Sciences.

Havström M., Callaghan T.V. & Jonasson S. (1993) Differential growth responses of *Cassiope tetragona*, an arctic dwarf-shrub, to environmental perturbations among three contrasting high- and sub-arctic sites. *Oikos* **66,** 389–402.

Higuchi H., Sakuratani T. & Utsunomiya N. (1999) Photosynthesis, leaf morphology, and shoot growth as affected by temperatures in cherimoya (*Annona cherimola* Mill.) trees. *Scientia Horticulturae* **80,** 91–104.

IPCC (2013) *Climate Change 2013: The Physical Science Basis. Contribution of Working Group I to the Fifth Assessment Report of the Intergovernmental Panal on Climate Change* (eds T.F. Stocker, D. Qin, G.-K. Plattner, M. Tignor, S.K. Allen, J. Boschung, . . . P.M. Midgley), pp. 1535. Cambridge University Press, New York, NY, USA.

Jardine K.J., Meyers K., Abrell L., Alves E.G., Serrano A.M.Y., Kesselmeier J., . . . Vickers C. (2013) Emissions of putative isoprene oxidation products from mango branches under abiotic stress. *Journal of Experimental Botany* **64,** 3697–3709.

Kivimäenpää M., Sutinen S., Calatayud V. & Sanz M.J. (2010) Visible and microscopic needle alterations of mature Aleppo pine (*Pinus halepensis*) trees growing on an ozone gradient in eastern Spain. *Tree Physiology* **30,** 541–554.

Kulmala M., Nieminen T., Chellapermal R., Makkonen R., Bäck J. & Kerminen V.M. (2013) Climate feedbacks linking the increasing atmospheric CO_2 concentration, BVOC emissions, aerosols and clouds in forest ecosystems. In *Biology, Controls and Models of Tree Volatile Organic Compound Emissions* (eds Ü. Niinemets & R.K. Monson), pp. 489–508. Springer, Berlin.

Laothawornkitkul J., Taylor J.E., Paul N.D. & Hewitt C.N. (2009) Biogenic volatile organic compounds in the Earth system. *The New Phytologist* **183,** 27–51.

Larcher W. (2003) *Physiological Plant Ecology. Ecophysiology and Stress Physiology of Fuctional Groups*, 4th edn. Springer, Berlin. 513 pp.

Li Z. & Sharkey T.D. (2013) Molecular and pathway controls on biogenic volatile organic compound emissions. In *Biology, Controls and Models of Tree Volatile Organic Compound Emissions* (eds Ü. Niinemets & R.K. Monson), pp. 119–151. Springer, Berlin.

Loreto F. & Schnitzler J. (2010) Abiotic stresses and induced BVOCs. *Trends in Plant Science* **15,** 154–166.

Luomala E.M., Laitinen K., Sutinen S., Kellomäki S. & Vapaavuori E. (2005) Stomatal density, anatomy and nutrient concentrations of Scots pine needles are affected by elevated CO2 and temperature. *Plant, Cell & Environment* **28,** 733–749.

Marques A.R., Garcia Q.S. & Fernandes G.W. (1999) Effects of sun and shade on leaf structure and sclerophylly of *Sebastiania myrtilloides* (Euphorbiaceae) from Serra do cipó, Minas Gerais, Brazil. *Boletim do Instituto de Botanica* **18,** 21–27.

Michelsen A., Rinnan R. & Jonasson S. (2012) Two decades of experimental manipulations of heaths and forest understory in the subarctic. *Ambio* **41,** 218–230.

Monson R.K. & Baldocchi D. (2014a) Fluxes of biogenic volatile compounds between plants and the atmosphere. In *Terrestrial Biosphere-Atmosphere Fluxes*, pp. 395–414. Cambridge University Press, New York, NY, USA.

Monson R.K. & Baldocchi D. (2014b) Leaf structure and function. In *Terrestrial Biosphere-Atmosphere Fluxes*, pp. 173–202. Cambridge University Press, New York, NY, USA.

Niinemets Ü. & Reichstein M. (2003) Controls on the emission of plant volatiles through stomata: differential sensitivity of emission rates to stomatal closure explained. *Journal of Geophysical Research. Atmospheres: JGR* **108,** ACH 1–17.

Niinemets Ü., Loreto F. & Reichstein M. (2004) Physiological and physicochemical controls on foliar volatile organic compound emissions. *Trends in Plant Science* **9,** 180–186.

Niinemets Ü., Kuhn U., Harley P.C., Staudt M., Arneth A., Cescatti A., . . . Peñuelas P. (2011) Estimations of isoprenoid emission capacity from enclosure studies: measurements, data processing, quality and standardized measurement protocols. *Biogeosciences* **8,** 2209–2246.

Niinemets Ü., Fares S., Harley P. & Jardine K.J. (2014) Bidirectional exchange of biogenic volatiles with vegetation: emission sources, reactions, breakdown an deposition. *Plant, Cell & Environment* **8,** 1790–1809.

Noe S.M., Copolovici L., Niinemets Ü. & Vaino E. (2008) Foliar limonene uptake scales positively with leaf lipid content: 'non-emitting' species absorb and release monoterpenes. *Plant Biology* **10,** 129–137.

Ortega J. & Helmig D. (2008) Approaches for quantifying reactive and low-volatility biogenic organic compound emissions by vegetation enclosure techniques – part A. *Chemosphere* **72,** 343–364.

Peñuelas J. & Staudt M. (2010) BVOCs and global change. *Trends in Plant Science* **15,** 133–144.

Popp M., Mirré V. & Brochmann C. (2011) A single Mid-Pleistocene long-distance dispersal by a bird can explain the extreme bipolar disjunction in crowberries (*Empetrum*). *Proceedings of the National Academy of Sciences* **108,** 6520–6525.

Possell M. & Loreto F. (2013) The role of volatile organic compounds in plant resistance to abiotic stresses: responses and mechanisms. In *Biology, Controls and Models of Tree Volatile Organic Compound Emissions* (eds Ü. Niinemets & R.K. Monson), pp. 209–235. Springer, Berlin.

Potosnak M.J., Baker B.M., LeStourgeon L., Disher S.M., Griffin K.L., Bret-Harte M.S. & Starr G. (2013) Isoprene emissions from a tundra ecosystem. *Biogeosciences* **10,** 871–889.

Rasulov B., Bichele I., Hüve K., Vislap V. & Niinements Ü. (2014) Acclimation of isoprene emission and photosynthesis to growth temperature in hybrid aspen: resolving structural and physiological controls. *Plant, Cell & Environment* **38,** 751–766.

Rinnan R., Rinnan Å., Faubert P., Tiiva P., Holopainen J.K. & Michelsen A. (2011) Few long-term effects of simulated climate change on volatile organic compound emissions and leaf chemistry of three subarctic dwarf shrubs. *Environmental and Experimental Botany* **72,** 377–386.

Rinnan R., Steinke M., McGenity T. & Loreto F. (2014) Plant volatiles in extreme terrestrial and marine environments. *Plant, Cell & Environment* **37,** 1776–1789.

Schollert M., Burchard S., Faubert P., Michelsen A. & Rinnan R. (2014) Biogenic volatile organic compound emissions in four vegetation types in high arctic Greenland. *Polar Biology* **37,** 237–249.

Stanhill G. & Cohen S. (2001) Global dimming: a review of the evidence for a widespread and significant reduction in global radiation with discussion of

its probable causes and possible agricultural consequences. *Agricultural and Forest Meteorology* **107,** 255–278.
Stewart-Jones A. & Poppy G. (2006) Comparison of glass vessels and plastic bags for enclosing living plant parts for headspace analysis. *Journal of Chemical Ecology* **32,** 845–864.
Tiiva P., Faubert P., Michelsen A., Holopainen T., Holopainen J.K. & Rinnan R. (2008) Climatic warming increases isoprene emission from a subarctic heath. *The New Phytologist* **180,** 853–863.
Vickers C.E., Gershenzon J., Lerdau M.T. & Loreto F. (2009) A unified mechanism of action for volatile isoprenoids in plant abiotic stress. *Nature Chemical Biology* **5,** 283–291.
Walker M.D., Wahren C.H., Hollister R.D., Henry G.H.R., Ahlquist L.E., Alatalo J.M., . . . Wookey P.A. (2006) From the cover: plant community responses to experimental warming across the tundra biome. *Proceedings of the National Academy of Sciences* **103,** 1342–1346.
Weijers S., Alsos I.G., Eidesen P.B., Broekman R., Loonen M.J.J.E. & Rozema J. (2012) No divergence in *Cassiope tetragona*: persistence of growth response along a latitudinal temperature gradient and under multi-year experimental warming. *Annals of Botany* **110,** 653–665.

Received 6 January 2015; received in revised form 20 February 2015; accepted for publication 23 February 2015

SUPPORTING INFORMATION

Additional Supporting Information may be found in the online version of this article at the publisher's web-site:

Figure S1. Experimental set-up in (a) Abisko, Northern Sweden on June 13, 2012 and (b) in *Cassiope tetragona*-dominated heath in Zackenberg, Northeast Greenland after snowmelt on July 4, 2012. Photos by Hanna M. Valolahti and Michelle Schollert.

Figure S2. Individual plant shoots of (a) *Cassiope tetragona* on July 17, 2012 and (b) *Salix arctica* on August 13, 2012 in Zackenberg, Northeast Greenland. Photos by Tora F. Nielsen.

Figure S3. Regression coefficients of a PLS model for the various leaf anatomy variables affecting (a) oxygenated monoterpenes (oMTs), (b) non-oxygenated monoterpenes (MTs), (c) sesquiterpenes (SQTs), (d) other reactive volatile organic compounds (ORVOCs) and (e) other volatile organic compounds (OVOCs). Error bars indicate ± 2 standard deviations of the regression coefficients. When the error bar does not include zero, the variable has a significant contribution in explaining the emission of the respective BVOC group.

Table S1. Leaf anatomy variables of (a) *Empetrum hermaphroditum* (b) *Cassiope tetragona* and (c) *Betula nana* from Abisko. All tested variables are shown. Values are means (±SE; $n = 4$–6). Arrows indicate a decrease or increase compared with the control (†$P < 0.1$; *$P < 0.05$).

Table S2. Leaf anatomy variables of (a) *Salix arctica* and (b) *Cassiope tetragona* from Zackenberg. All tested variables are shown. Values are means (±SE; $n = 3$–5). Arrows indicate a decrease or increase compared with the control (†$P < 0.1$; *$P < 0.05$).

Table S3. Mean BVOC emissions (μg g^{-1} h^{-1}; ± SE; $n = 4$–6) from (a) *Empetrum hermaphroditum*, (b) *Cassiope tetragona* and (c) *Betula nana* in a long-term field experiment with control (C), shading (S) and warming (W) treatments in Abisko. BVOCs are divided into isoprene, non-oxygenated monoterpenes (MTs), oxygenated monoterpenes (oMTs), sesquiterpenes (SQTs), other reactive volatile organic compounds (ORVOCs) and other volatile organic compounds (OVOCs). *P*-values from mixed models for each of the groups across the campaigns are shown in the bottom row when $P < 0.1$. Significant differences from the control (C) treatment within a campaign are indicated next to the values for the shading (S) and warming (W) treatments.

Table S4. Mean BVOC emissions (μg g^{-1} h^{-1}; ± SE; $n = 4$–6) from (a) *Salix arctica*, (b) *Cassiope tetragona* measured in long-term field experiments with control (C), shading (S), and warming (W) treatments in Zackenberg. BVOCs are divided into isoprene, non-oxygenated monoterpenes (MTs), oxygenated MTs (oMTs), sesquiterpenes (SQTs), other reactive volatile organic compounds (ORVOCs) and other volatile organic compounds (OVOCs). *P*-values from mixed models for each of the groups across the campaigns are shown in the bottom row when $P < 0.1$. Significant differences from the control (C) treatment within a campaign are indicated next to the values for the shading (S) and warming (W) treatments.

Table S5. Mean emission potentials (μg g^{-1} h^{-1}; ± SE; $n = 3$–6) of isoprene, oxygenated monoterpenes (oMTs), non-oxygenated monoterpenes (MTs) and sesquiterpenes (SQTs) for (a) *Empetrum hermaphroditum*, *Cassiope tetragona* (Abisko), *Betula nana* and (b) *Salix arctica* and *C. tetragona* (Zackenberg) in control (C), shading (S) and warming (W) treatments. The emission potentials were calculated according to Guenther (1993) for the temperature of 30 °C and the PPFD of 1000 μmol m^{-2} s^{-1} (for isoprene).

Table S6. Mean BVOC emissions (μg g^{-1} h^{-1}; ± SE; $n = 15$–18) of individual compounds grouped as isoprene, oxygenated monoterpenes (oMTs), non-oxygenated monoterpenes (MTs), sesquiterpenes (SQTs), other reactive volatile organic compounds (ORVOCs), and other volatile organic compounds (OVOCs) for (a) *Empetrum hermaphroditum* (b) *Cassiope tetragona* and (c) *Betula nana* from Abisko.

Table S7. Mean BVOC emissions (μg g^{-1} h^{-1}; ± SE; $n = 13$–15) of individual compounds grouped as isoprene, oxygenated monoterpenes (oMTs), non-oxygenated monoterpenes (MTs), sesquiterpenes (SQTs), other reactive volatile organic compounds (ORVOCs), and other volatile organic compounds (OVOCs) for (a) *Salix arctica* and (b) *Cassiope tetragona* from Zackenberg.